ELSEVIER

Thermochimica Acta 378 (2001) 69–77

thermochimica acta

www.elsevier.com/locate/tca

Solid state characterization of potential protozoocidal agents — aminoisoxazolylnaphthoquinones

Norma R. Sperandeo, María M. de Bertorello*

Departamento de Farmacia, Facultad de Ciencias Químicas, Universidad Nacional de Córdoba, Córdoba 5000, Argentina

Received 14 November 2000; received in revised form 11 April 2001; accepted 15 April 2001

Abstract

As part of their preformulation evaluation, four in vitro protozoocidal 3,4-dimethyl-5-isoxazolylnaphthoquinones (**ANQ-1–4**) were investigated by differential scanning calorimetry (DSC), simultaneous differential thermal analysis–thermogravimetry–derivative thermogravimetry (DTA–TG–DTG), and Fourier transform infrared spectroscopy (FTIR). X-ray powder diffractometry (XRPD), thermomicroscopy and polarized light microscopy were used as an aid to interpret the thermoanalytical curves. The study demonstrated that the compounds are crystalline solids, unaffected by oxygen, safely manipulated at room temperature (RT) and also at higher temperatures as solids; however, all decompose exothermically at about their mp. Polycrystalline mixtures or undesirable solvates were not detected. All the compounds are insoluble in water and *n*-hexane and slightly soluble in ethanol, indicating that all are candidates to improve their solubilities in order to avoid formulation problems.

Keywords: Isoxazolylnaphthoquinones; DSC; DTA–TG–DTG; X-ray powder diffractometry; Solubility

1. Introduction

Characterization and control of the solid state of drug substances are receiving increased attention by pharmaceutical companies and regulatory agencies because many substances crystallize in more than one crystal form. This fact may have a wide range of implications in the pharmaceutical field [1].

The different solid forms of a drug, for example, the solvates, hydrates, polymorphs and amorphous forms, may differ with respect from important pharmaceutical properties, such as solubility, dissolution rate, bioavailability, chemical and physical stability, shelf life and even in the therapeutic activity and toxicity [2]. Consequently, knowledge of the physical properties and crystal forms of a drug substance is essential for the development of a new medicine.

Previous studies [3,4] by thermal analysis and IR spectroscopy of nine isoxazolylnaphthoquinones, compounds which display important biological activities against *Staphylococcus aureus* [5,6] and *Trypanosoma cruzi* [7], provided us with enough information about their physical properties and different thermal behaviors in order to verify the absence of unwanted tautomeric mixtures in the samples submitted to biological assays.

As an extension of our research program, in the present work four new isoxazolylnaphthoquinones of the series (**ANQ-1–ANQ-4**) exhibiting significant in vitro activities against *T. cruzi*, *Trypanosoma brucei rhodediense* and *Leishmania donovani* [8] were examined by differential scanning calorimetry

* Corresponding author. Tel.: +54-51-334163; fax: +54-351-4334127.
E-mail address: marcor@dqo.fcq.unc.edu.ar (M.M. de Bertorello).

0040-6031/01/$ – see front matter
PII: S0040-6031(01)00569-X

(DSC), simultaneous differential thermal analysis–thermogravimetry–derivative thermogravimetry (DTA–TG–DTG), Fourier transform infrared spectroscopy (FTIR), X-ray powder diffractometry (XRPD), thermomicroscopy, polarized light microscopy and solubility. The aim of this study was to obtain a fairly complete profile of the solid forms of these new naphthoquinone derivatives, establishing appropriate specifications to assure their lot-to-lot conformity. We also demonstrated the utility of thermal analysis, especially DSC, both for the drug purity control of **ANQ-1**–**ANQ-4** and the assessment of their stabilities against heat and oxygen.

2. Experimental

2.1. Materials

3-Hydroxymethyl-*N*-hydroxymethyl-*N*-(3,4-dimethyl-5-isoxazolyl)-4-amino-1,2-naphthoquinone (**ANQ-1**), *N*-(3,4-dimethyl-5-isoxazolyl)-4-amino-1,2-naphthoquinone-2-one oxime (**ANQ-2**), *N*-(3,4-dimethyl-5-isoxazolyl)-4-amino-1,2-naphthoquinone-2-[*O*-(carboxymethyl)]-oxime (**ANQ-3**) and 2-(3,4-dimethyl-5-isoxazolylamino)-*N*-(3,4-dimethyl-5-isoxazolyl)-1,4-naphthoquinone-4-imine (**ANQ-4**) were prepared and purified to analytical grade [8,9]. The recrystallization procedure was the following: a hot saturated solution of drug in the appropriate solvent (**ANQ-1** and **ANQ-2** in methanol; **ANQ-3** in methanol–water (5:1) and **ANQ-4** in benzene–carbon tetrachloride (2:1)) was allowed to stand first at room temperature (RT) and then at -20°C. The separated crystals were next filtered and dried in vacuo.

For thin layer chromatography (TLC) analysis, precoated plates of silica gel 60 F_{254} (Merck) were used and spots were visualized with UV and daylight. Solvents of analytical reagent grade and distilled water were employed.

2.2. Thermal analysis

The DSC measurements were recorded on a Mettler TA 3000, DSC-30 cell equipped with a TC 10 processor, able to calculate peak temperatures and enthalpy values, and a Swiss Matrix print. DTA–TG–DTG scans were run on a simultaneous Netzsch STA 429 analyzer. The operating conditions in an open-pan system were as follows: (a) DSC: heating rate, 2°C min^{-1}, and static air; (b) DTA–TG–DTG: heating rate, 10°C min^{-1}, chart speed, 120 mm h^{-1} and dynamic N_2 (99.99%) atmosphere. The temperatures axis were calibrated with pure indium (mp: 156.60°C). Empty aluminium (DSC) and alumina (DTA–TG–DTG) pans were used as references. The reported values were at least the average of two independent measurements. The reproducibility in transition temperatures was $\pm 0.2^{\circ}$C (DSC) and $\pm 2^{\circ}$C (DTA: graphical determination).

2.3. Thermomicroscopy

The physical and morphological changes undergone by the samples during the process of heating were observed through a Kofler micro hot stage (Leitz, Wetzlar, Germany) at a constant rate from RT up to 280°C.

2.4. X-ray powder diffraction analysis

Powder diffraction patterns were recorded using an X-ray diffractometer (Phillips PW 1010) with Ni-filtered Cu Kα radiation and a goniometer speed of 1° (2θ)/min. Data were collected at room temperature from 2θ=0 to 70°.

2.5. Infrared spectroscopy

Infrared spectra (KBr pellets) were recorded on a FTIR spectrophotometer (Nicolet 5-SXC). The number of scans were 40 and the resolution was 8 cm^{-1}.

2.6. Birefringence measurements

The crystallinity of the compounds was assessed by measuring their birefringence according to the USP test of crystallinity [10]. Then, samples were suspended in silicone immersion oil and examined under a polarized light microscope equipped with cross polars.

2.7. Solubility measurements

The equilibrium solubilities of solutes was determined in *n*-hexane, absolute ethanol and distilled

water by adding an excess of solid to 10 ml of the tested solvent in 20 ml stoppered vials. The mixtures were mechanically shaken for 24 h at 25.0 ± 0.1°C (in a constant-temperature water bath regulated by a Haake F3 thermostat with ±0.1 precision). After that, the contents of the vials were filtered through sintered glasses to avoid contamination with the solids. An analytical UV–VIS spectrophotometric procedure was employed to measure solute concentration in a Shimadzu UV-260 spectrophotometer. Therefore, aliquots of the filtrate were suitably diluted in the assayed solvents to determine their absorbances using λ_{max} as analytical wavelength. Since the UV–VIS absorption spectra of **ANQ-1**–**ANQ-4** have three main bands, absorbances at each λ_{max} were determined and used for concentration calculations. For every compound, reference samples were adequately processed to obtain plots of absorbance against concentration. All the compounds showed adherence to Beer's law. Six determinations were made for each solvent and averaged. The solubility was expressed as milligram solute per gram of solvent (w/w).

3. Results and discussion

3.1. Physicochemical properties of the solids

Isoxazolylnaphthoquinones **1**–**4** (**ANQ-1**–**ANQ-4**) were characterized by DSC, DTA–TG–DTG or DTA–TG–DDTA, FTIR, thermomicroscopy, XRPD and birefringence measurements.

3.1.1. *ANQ-1* and *ANQ-4*

Thermoanalytical curves of **ANQ-1** are shown in Fig. 1. The DSC plot exhibited a small endothermic peak at 212.6°C attributable to a melting process, superimposed with a large exothermic effect at 217.2°C. No peaks were observed below these temperatures, pointing out the absence of methanol solvates or polymorphic mixtures. DTA–TG–DTG scans were used to complement these results. Thus, according to the TG curve, no weight losses were produced in the 50–200°C region, the mass loss (18%) coincided with the DTA endothermic–exothermic effects and it occurred in a sharp step between 204 and 235°C followed by a progressive weight loss that continued even at higher temperatures. From these results, it is

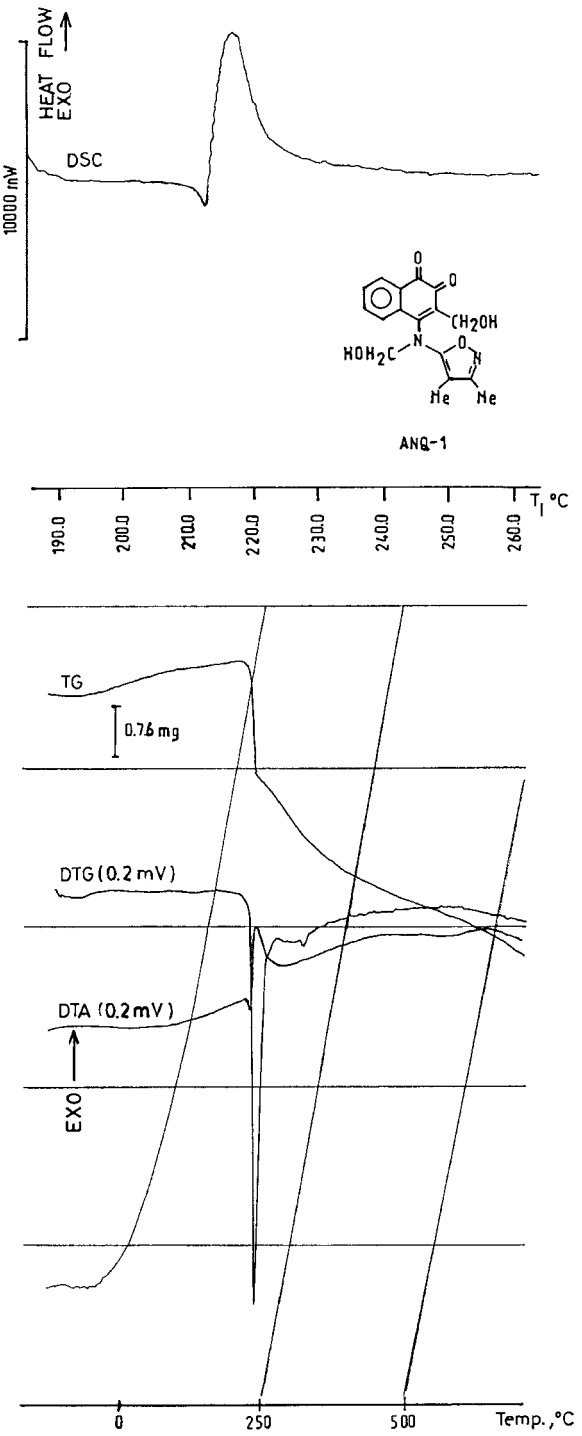

Fig. 1. DSC and DTA–TG–DTG curves of 3-hydroxymethyl-*N*-hydroxymethyl-*N*-(3,4-diMe-5-isoxazolyl)-4-amino-1,2-naphthoquinone (**ANQ-1**).

evident that melting started but subsequent rapid decomposition took place.

The sequence of thermal events of Fig. 1 was confirmed by observations under the hot stage. Upon heating from RT to 210°C phase modifications and evaporation losses were not detected. The yellow crystalline fibers began to melt at about 215°C; concurrently the cover glass slightly blurred and tiny bubbles appeared, indicating a vaporization process of volatile products produced by a thermal decomposition reaction. The crystalline particles melted completely at ca. 217°C and upon further heating the melted droplets changed in size and darkened, showing that decomposition continued in the melted phase. It is interesting to note that this thermal behavior is similar to that observed for other two isoxazolylnaphthoquinones which have OH-substituents near a quinonic C=O group [3]. As stated, such behavior can be explained assuming the predominance of intermolecular interactions in solid phase causing a compound to decompose while melting [3,11]. **ANQ-1** has two OH, one near the 2-C=O group, making the formation of strong inter and intramolecular hydrogen-bonds possible. Its IR spectrum (not shown) supports this assumption about the structure since it exhibited no bands in the region of free OH (3650–3590 cm^{-1}). The two hydroxyl bands appeared at 3329 and 3281 cm^{-1} indicating OH groups associated through hydrogen bondings. In addition, the two CO absorption bands were observed at 1676 and 1628 cm^{-1}, as expected for conjugated CO groups.

The thermoanalytical curves of **ANQ-4** (not shown) are similar to those of **ANQ-1** (Fig. 1). No weight losses or peaks due to solvent removal or polycrystalline mixtures were observed in the DSC and DTA–DDTA–TG curves. Microscopic observation under the Kofler indicated that the red prismatic crystals of **ANQ-4** started to melt at 205°C and liquefied completely at about 207°C. Simultaneously, the cover slip showed little bubbles. The molten phase changed in size and darkened, indicating that the thermal decomposition continued in the melt. This thermal behavior was expected since **ANQ-4** possesses an –NH group near a C=O group capable of forming hydrogen-bondings, which in turn may lead to the predominance of intermolecular interactions in solid state. Its IR spectrum (not shown) indicated the occurrence of associates in solid state since there are no peaks between 3500 and 3350 cm^{-1}, region of free NH forms. The NH and the CO absorption bands appeared at 3309 and 1656 cm^{-1}, respectively, which are normal positions of hydrogen-bonded NH and conjugated CO groups.

3.1.2. *ANQ-2 and ANQ-3*

Fig. 2 display the DSC and DTA–DDTA–TG traces of **ANQ-2**. As it is shown, the DSC curve exhibited no desolvation or melting peaks. There is only a single sharp exothermic peak attributable to a thermal decomposition reaction. The DTA–DDTA–TG curves corroborated the DSC behavior. The TG scan showed no solvent loss up to 200°C which in addition to the elemental analyses data (UMYNFOR, Bs. Aires) ratified the absence of undesirable solvates. The weight change is associated with the DTA exothermic effect and occurred as a sharp mass loss (12%) between 200 and 227°C. Also, a gradual weight loss from 227°C and above was observed.

The thermal characterization of **ANQ-3** deserves to be briefly commented. The trace (a) of Fig. 3 corresponds to the DSC curve of a crystallized sample whose purity was checked by TLC which did not reveal impurities. Then, the small shoulder on the left-hand side of the exothermic peak (198.5°C) was overlooked. Yet, when the elemental analysis failed, the shoulder was reviewed. As a consequence, a portion of **ANQ-3** was purified by column chromatography on silica gel (isolating as unique impurity a little amount of **ANQ-2**, its synthetic precursor) and recrystallization from methanol/water. Subsequently, the purified sample was analyzed by HPLC (Konik instrument; RP_{18} column, methanol–H_2O (50:50, v/v) as elution solvent), revealing no impurities. A new DSC plot (Fig. 3, trace (b)) and the DTA–DDTA–TG curves confirm the absence of shoulders and showed that the DSC exothermic peak had shifted to 203.5. These results clearly highlight the importance of DSC for the purity control of these compounds.

The possibility that the exothermic effects observed in Figs. 2 and 3 were due to an amorphous-to-crystalline transition known [12] to be irreversible and evidenced by exothermic peaks, was discarded considering the results of the USP test for crystallinity [10] and the observations under the Kofler. Thus, microscopic observations under polarized light indicated that **ANQ-2** and **ANQ-3** are both crystalline

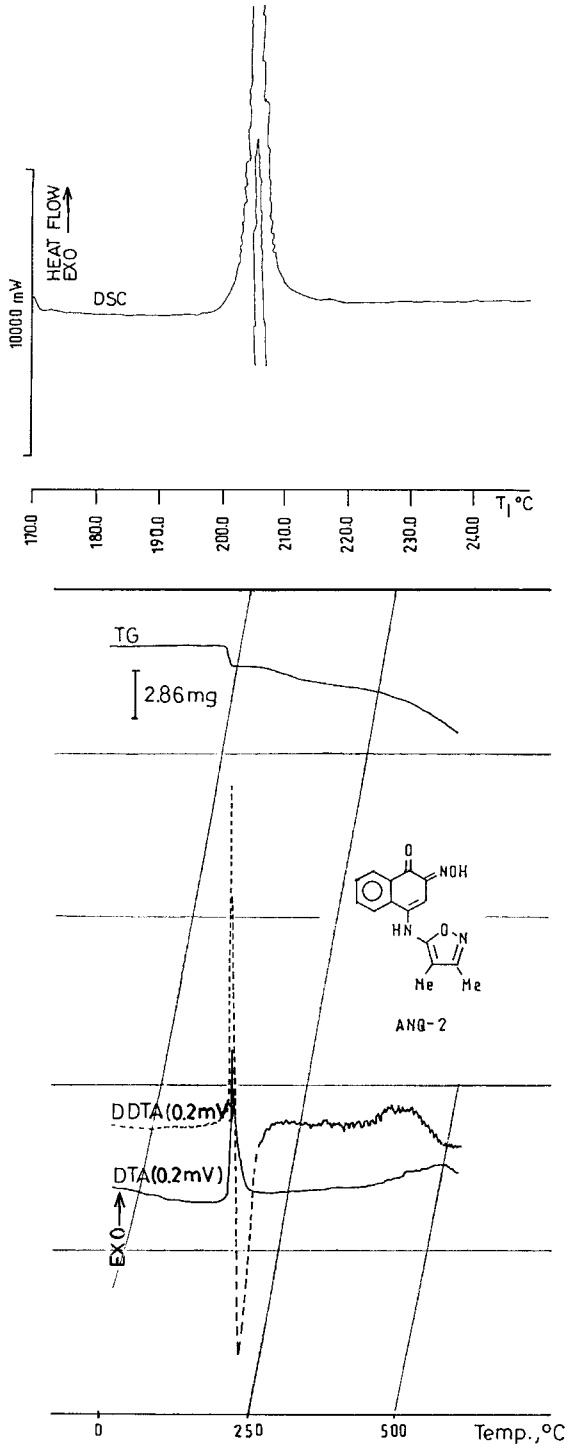

Fig. 2. DSC and DTA–DDTA–TG plots of *N*-(3,4-diMe-5-isoxazolyl)-4-amino-1,2-naphthoquinone-2-one oxime (**ANQ-2**).

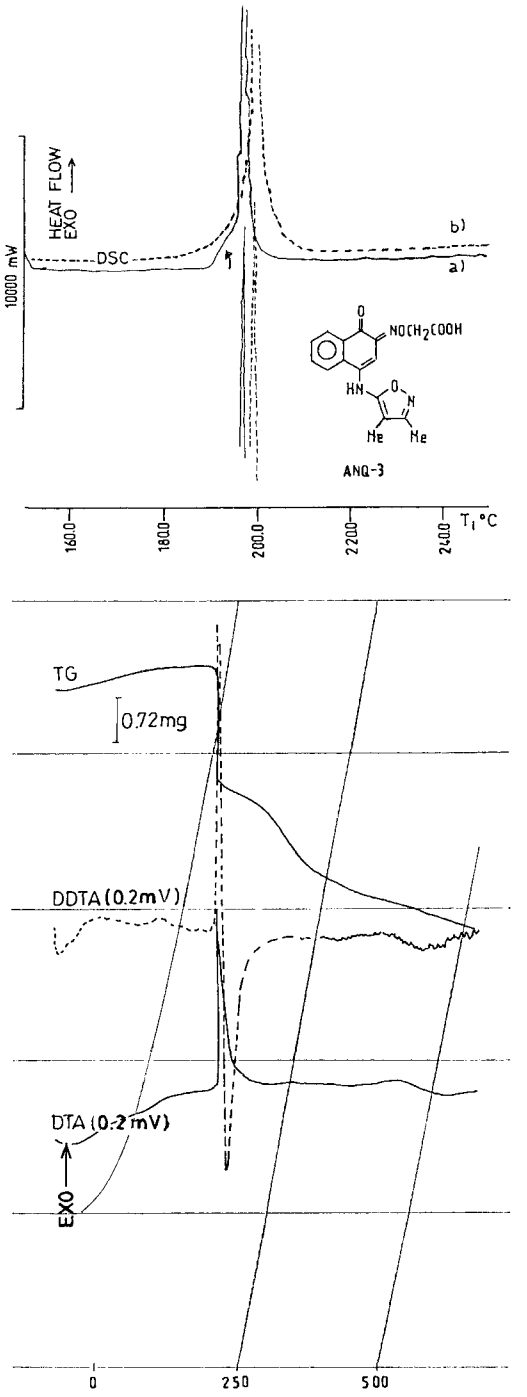

Fig. 3. DSC (a) initial sample, (b) purified sample and DTA–DDTA–TG (purified sample) plots of *N*-(3,4-diMe-5-isoxazolyl)-4-amino-1,2- naphthoquinone-2-[*O*-(carboxymethyl)]-oxime (**ANQ-3**).

trimetric solids. The first appeared euhedron yellow plate-shaped with birefringence (green, 2° order) and extinction at 17° (at the side of grain); while the second, euhedron light yellow fiber-shaped with birefringence (about 2° order, the exact interference color could not be discerned because the material had altered its surface) and oblique extinction at 40° (at maximum longitude of fiber), respectively.

On the other hand, heating of **ANQ-2** and **ANQ-3** on the hot stage showed that both compounds decomposed, starting the decomposition reaction before the crystalline particles melted. In fact, at a few degrees

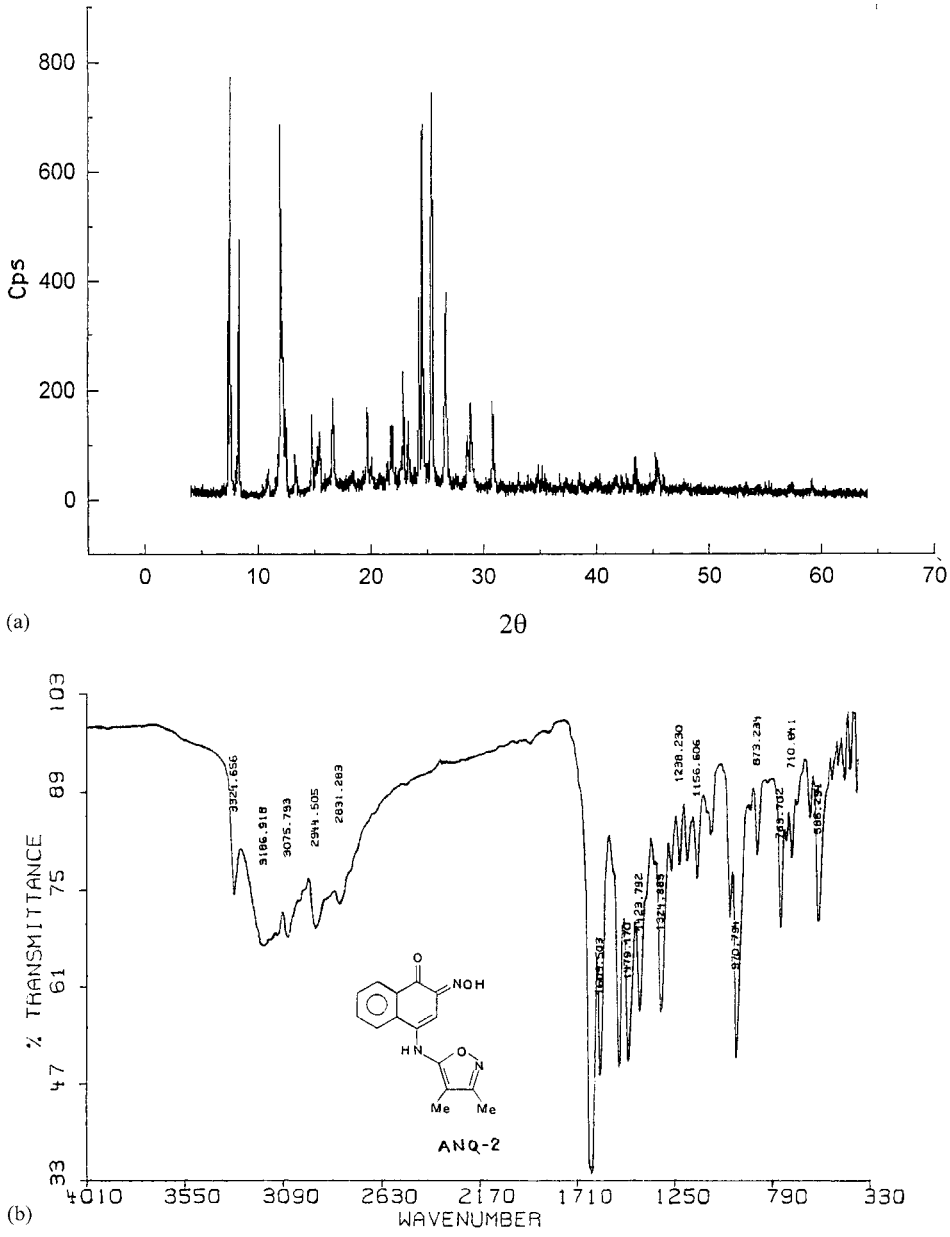

Fig. 4. (a) XRPD pattern and (b) IR spectrum (KBr) of *N*-(3,4-diMe-5-isoxazolyl)-4-amino-1,2-naphthoquinone-2-one oxime (**ANQ-2**).

below their melting points, the cover glass began to blur and then, little bubbles were observed indicating evaporation loss due to a thermal decomposition process. Upon further heating the crystals melted and decomposition continued at an increased rate; the quantity of bubbles in the cover increased in such a way that it was necessary to take out the cover slip to see the dark melted droplets.

To confirm conclusively that **ANQ-2** and **ANQ-3** were crystalline compounds, their XRPD patterns were obtained. As it can be seen in Figs. 4a and 5a, they exhibited several well-resolved sharp peaks; there are no broad humps between 2° and 20° (2θ value) as amorphous forms have showing that both compounds are crystalline solids and have different crystal structures. FTIR spectroscopy also supports these findings

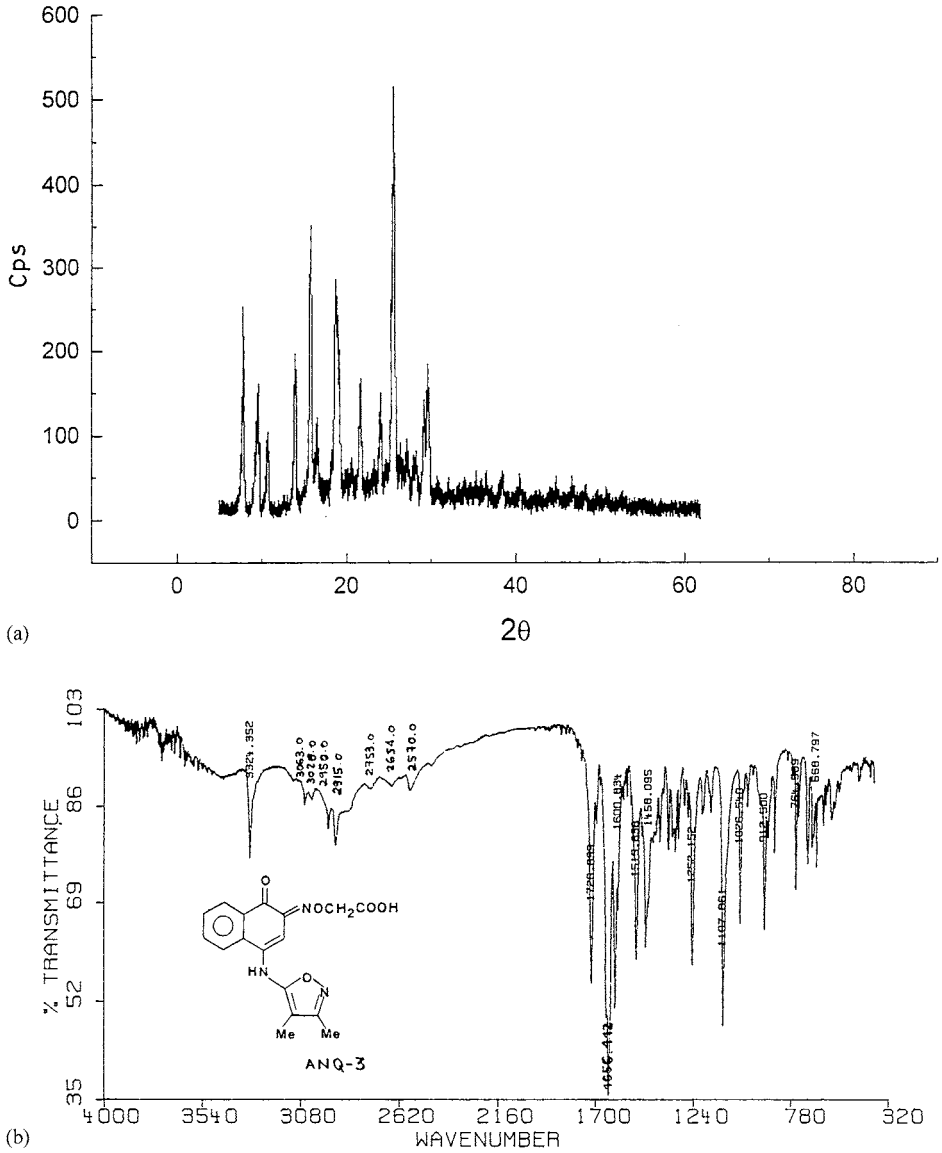

Fig. 5. (a) XRPD pattern and (b) IR spectrum (KBr) of *N*-(3,4-diMe-5-isoxazolyl)-4-amino-1,2- naphthoquinone-2-[*O*-(carboxymethyl)]-oxime (**ANQ-3**).

since both IR spectra (Figs. 4b and 5b) showed sharp instead of broad peaks.

In addition, the thermal decomposition reaction was investigated by heating samples of **ANQ-2** and **ANQ-3** in a heating bath up to their melting points; cooling and analyzing the dark residues formed by TLC. Chromatograms showed several spots but none of them corresponded to the intact drugs, indicating a total thermal decomposition.

As a result, the DSC and DTA exothermic peaks of **ANQ-2** and **ANQ-3** could not be attributed to an amorphous-to-crystalline transition. The absence of melting peaks can be explained considering that melting was not an isolated event from the thermal response as regards the exothermic decomposition reaction. As it was identified by the Kofler, melting does occur but during decomposition and not before. Then, as DSC and DTA measurements are based on total heat flux, [13] melting peaks were not observed in either curves.

3.2. Thermal–oxidative stability: preliminary studies

It is widely known that several compounds deteriorate during storage or manipulation in an oxidizing atmosphere, hence from the viewpoint of pharmaceutics the evaluation of the stability of a sample against heat and an oxidative atmosphere is a matter of importance. DSC data provided a valuable aid in assessing such stability since the higher the extrapolated onset (t_{onset}) and peak maximum temperatures (t_{max}), the more the thermal–oxidative stability of a sample [14,15]. DSC thermal parameters (t_{onset}, t_{max} and heats of transitions (ΔH)) for **ANQ-1–4** are listed in Table 1. As it was stated, none of the compounds studied were found undergoing a true melting process; instead they decomposed exothermically, hence the reported ΔH values were all negative.

Temperatures, t_{onset} and t_{max} of **ANQ-1–4** can be used as primary parameters of their resistance to thermal–oxidative decomposition. Thus, **ANQ-1–4** have t_{onset} higher than 180°C, decreasing their stability in the sequence **ANQ-1** > **ANQ-2** > **ANQ-3** > **ANQ-4**. According to these results, the four compounds are stable at high temperatures as solids, but near their melting points they are unstable and experiment thermal decomposition reactions.

Moreover, as it was seen in Figs. 1–3, **ANQ-1–4** displayed similar thermal behaviors in air (DSC curves) and in a non-oxidizing atmosphere such as N_2 (DTA curves). The number of the peaks and their shapes were similar, but the DTA curves were shifted to higher temperatures due to their higher heating rate. This observation clearly remarked that the atmosphere had no effect on thermal decomposition of **ANQ-1–4**. Consequently, all the compounds studied are unaffected by oxygen. Then, they can be safely manipulated in air at RT and even at higher temperatures. Consistently, samples stored 2 years at RT did not present decomposition products as indicated by TLC and DSC analyses.

3.3. Solubility properties

The equilibrium solubilities of **ANQ-1–4** in *n*-hexane, absolute ethanol and water at 25°C are collected in Table 2. Despite the equilibrium was attained within

Table 1
DSC data on the thermal behavior of **ANQ-1–ANQ-4**

Compound	DSC (°C)						
	MW	Mp[a] (°C, decomposition)	Onset	Peak (endothermic)	Peak (exothermic)	ΔH (J g^{-1})	Weight (mg)
ANQ-1	328.32	225–226	211.0	212.6	217.2	−475.9	1.998
ANQ-2	283.29	211–212	204.4	–	205.2	−839.4	3.125
ANQ-3[b]	341.32	196–197	189.3	–	198.5	−886.1	1.011
ANQ-3[c]	341.32	197–198	193.0	–	203.5	−1830.6	1.210
ANQ-4	362.39	206–207	198.5	199.3	206.0	−745.2	4.135

[a] Büchi apparatus, uncorrected.
[b] Initial sample.
[c] Purified sample.

Table 2
Solubilities of **ANQ-1–4** at 25.0°C in selected solvents

Compound	Solubility (mg g^{-1})		
	Distilled water	Ethanol	*n*-Hexane
ANQ-1	Insoluble	2.54	Insoluble
ANQ-2	Insoluble	2.13	Insoluble
ANQ-3	Insoluble	1.89	Insoluble
ANQ-4	Insoluble	0.44	Insoluble

24 h, all the derivatives remained stable during the determination, as indicated by TLC and UV analysis. As it can be seen, the compounds are insoluble in water and *n*-hexane, and slightly soluble in ethanol (0.44–2.54 mg g^{-1} (w/w)). These solubility characteristics are a serious limitation which can restrict their biological efficacy and render **ANQ-1–4** candidates for improving their solubilities.

4. Conclusions

The data reported in this article provided a meaningful set of solid state characteristics of **ANQ-1–4**, ensuring their quality and sample-to-sample reproducibility. They also confirmed the utility of DSC, at the earliest stages of drug development, as a useful tool for: solving delicate preformulation problems such as the recognition of solvates unsuitable as drugs, for instance, methanol or benzene solvates which were discarded from these compounds; checking the validity of the results obtained by other purity assays such as TLC, as it was demonstrated in the case of **ANQ-3**; and confirming that in the purification conditions employed, the samples are single crystal forms not polycrystalline mixtures.

Furthermore, the equilibrium solubilities determined provide useful indication of the necessity to perform subsequent systematic studies in order to optimize the unfavorable solubility characteristics of these potential protozoocidal agents.

Acknowledgements

This work was supported by the Consejo de Investigaciones Científicas y Tecnológicas de la Provincia de Córdoba (CONICOR), the Secretaría de Ciencia y Técnica de la Univ. Nac. de Cba (SECYT) and the Consejo Nacional de Investigaciones Científicas y Técnicas (CONICET) of the Republic of Argentina. The authors also thank Eng. Martín Portela (C.I.M.M.) for recording DTA–TG–DTG curves and Dr. J. L. Castañeda (INTEC, Pcia. de Sta. Fe) for recording DSC curves.

References

[1] S.R. Byrn, R. Pfeiffer, M. Ganey, C. Hoiberg, G. Poochikian, Pharm. Res. 12 (1995) 945.
[2] S.R. Byrn, R. Pfeifer, J.F. Stowell, Solid-State Chemistry of Drugs, 2nd Edition, SSCI Inc., West Lafayette, IN, 1999 (Chapter 1).
[3] N.R. Sperandeo, M.M. de Bertorello, J. Therm. Anal. 39 (1993) 1311.
[4] N.R. Sperandeo, C.V. Mattia, M.M. de Bertorello, J. Therm. Anal. 43 (1997) 267.
[5] P. Bogdanov, I. Albesa, N.R. Sperandeo, C. Luna, M.M. de Bertorello, Experientia 52 (1996) 600.
[6] P. Bogdanov, I. Albesa, A. Eraso, N.R. Sperandeo, M.M. de Bertorello, J. Appl. Bacteriol. 78 (1995) 73.
[7] P. Amuchástegui, E. Moretti, B. Basso, N.R. Sperandeo, M.M. de Bertorello, M.C. Briñón, J. Protozool. 37 (1990) 15A–89A.
[8] N.R. Sperandeo, M.M. de Bertorello, M.C. Briñón, Eur. J. Med. Chem., submitted for publication.
[9] M.R. Longhi, M.M. de Bertorello, M.C. Briñón, J. Pharm. Sci. 78 (1988) 408.
[10] U.S.P. XXIII, 695, p. 1790.
[11] T. Halasi, J. Balla, J. Therm. Anal. 37 (1991) 829.
[12] D. Dollimore, Thermochim. Acta 203 (1992) 7.
[13] A.K. Galwey, J. Therm. Anal. 41 (1994) 267.
[14] W.W.M. Wendlandt, in: P.J. Elving, I.M. Kolthoff (Eds.), Thermal Methods of Analysis (Chemical Analysis Series No. 19), Monographs on Analytical Chemistry and Applications, 2nd Edition, Wiley, New York, 1974, p. 6.
[15] B. Kowalski, Thermochim. Acta 184 (1991) 49.